

Dimerization-induced enhancement of the spin gap in the quarter-filled two-leg rectangular ladder

Y. Yan and S. Mazumdar

Department of Physics, University of Arizona, Tucson, AZ 85721

S. Ramasesha

*Solid State and Structural Chemistry Unit,
Indian Institute of Science, Bangalore 560 012, India*

(Dated: June 15, 2018)

Abstract

We report density-matrix renormalization group calculations of spin gaps in the quarter-filled correlated two-leg rectangular ladder with bond-dimerization along the legs of the ladder. In the small rung-coupling region, dimerization along the leg bonds can lead to large enhancement of the spin gap. Electron-electron interactions further enhance the spin gap, which is nonzero for all values of the rung electron hopping and for arbitrarily small bond-dimerization. Very large spin gaps, as are found experimentally in quarter-filled band organic charge-transfer solids with coupled pairs of quasi-one-dimensional stacks, however, occur within the model only for large dimerization and rung electron hopping that are nearly equal to the hopping along the legs. Coexistence of charge order and spin gap is also possible within the model for not too large intersite Coulomb interaction.

PACS numbers: 71.10.Fd, 71.30.+h, 71.27.+a, 75.10.Pq

I. INTRODUCTION

Coupled pairs of one-dimensional (1D) chains, referred to as two-leg ladders, have been widely investigated within the spin 1/2 antiferromagnetic Heisenberg Hamiltonian because they exhibit behavior different from both the isolated 1D chain as well as the two-dimensional (2D) lattice. Ignoring electron occupations, two different kinds of couplings between the 1D chains, as shown in Figs. 1(a) and (b), have been of interest. We refer to the system of Fig. 1(a) as a rectangular ladder and that of Fig. 1(b) as a zigzag ladder. Within the spin 1/2 Heisenberg Hamiltonian for the rectangular ladder, the energy gap between the lowest spin triplet ($S=1$) excitation and the spin singlet ($S=0$) ground state, hereafter the spin gap, is nonzero for arbitrarily small spin exchange along the rung bonds.^{1,2,3,4} The zigzag ladder of Fig. 1(b) can also be considered as a 1D chain with the interstack (intrastack) couplings corresponding to the nearest neighbor (next nearest neighbor) couplings in the 1D chain. The spin gap in the antiferromagnetic zigzag ladder is nonzero only for the intrastack spin exchange above a critical value^{5,6,7,8}. Nonzero spin gap is also found in the 1/2-filled band rectangular ladder within the Hubbard Hamiltonian with finite on-site electron-electron (e-e) interaction.^{3,9} Spin gaps and superconducting pair-pair correlation functions in weakly doped rectangular ladders have been investigated within Hubbard and t-J models³.

The strong interest in the theory of undoped and weakly doped 1/2-filled band ladders owes its origin to possible connections with theories of high temperature superconductivity in the cuprates¹⁰. Whether or not significant spin gap occurs in ladder structures at other commensurate bandfillings is also an interesting question. The particular commensurate bandfilling that has been investigated so far is 1/4. Exact diagonalization studies of finite 1/4-filled rectangular ladders with e-e and Holstein electron-phonon (e-p) interactions have demonstrated the coexistence of charge-order and spin-Peierls states¹². The magnitude of the spin gap in the thermodynamic limit due to such a transition was not calculated. Density matrix renormalization group (DMRG) calculations for the rectangular ladder within an extended Hubbard Hamiltonian with repulsive on-site interaction U and nearest neighbor interaction V have shown that the checkerboard charge-ordering of Fig. 1(c) occurs only for V larger than a critical value $V_c(U)$ ¹¹. The calculated spin gaps in the thermodynamic limit, obtained from extrapolations, are nonzero for $t_\perp < t$, where t_\perp and t are the one-electron hopping parameters along the ladder rungs and legs, respectively, in agreement with weak

coupling renormalization group calculations¹³. The magnitudes of the extrapolated spin gaps are, however, tiny. Furthermore, the uncertainties in the extrapolated spin gaps are rather large in this parameter regime due to finite-size effects, and are comparable to the magnitudes of the spin gaps.^{9,11} For example, for $U = 8$, $V = 0$ and hopping parameter $t_{\perp} = 0.7$ (all in units of t) the spin gap is $\sim 0.03 \pm 0.01$, while for the same U and hopping parameter t_{\perp} but $V = 2$, the spin gap is $\sim 0.01 \pm 0.005$. The spin gap also goes to 0 for hopping parameter $t_{\perp} \geq t$, and consequently, significant spin gap is absent in the regular rectangular 1/4-filled band ladder for repulsive $U > V$. Significant spin gap does occur in the zigzag 1/4-filled band electron ladder with both e-e and e-p interactions. For $t_d > 0.5858t_s$ the ground state is a Bond-Charge-Density wave (BCDW) (see Fig. 1(d)) with coupled lattice distortion, charge order and very large spin gap.¹⁴

Experimentally, large spin gaps have been observed at low temperatures in several recently discovered organic charge-transfer solids with strong pairwise couplings between quasi-1D stacks of organic molecules, and weak interpair couplings^{15,16,17,18}. In all cases, there occurs first a metal-insulator transition at high temperature that is accompanied by leg bond-dimerization, following which there occurs an insulator-insulator transition which is accompanied by the opening of a spin gap. The temperatures T_{SG} at which the spin gap transitions occur, ~ 70 K in the charge-transfer solid $(DT\text{-}TTF)_2[\text{Au}(\text{mnt})_2]$ ¹⁵, and ~ 170 K in $(BDT\text{FP})_2\text{PF}_6(\text{PhCl})_{0.5}$ ¹⁸, are unusually high compared to the spin-Peierls transition temperatures $T_{SP} \sim 15\text{--}20$ K in the 1D 1/4-filled band charge-transfer solids^{19,20}.

The very large T_{SG} in the the coupled-stack systems suggest that the mechanism by which the gap opens is probably unrelated to the intrachain spin-Peierls transition, which in the 1/4-filled band is tetramerization, or dimerization of the dimerization.²⁰ Based on the experimentally observed high temperature dimerization, the ladder model of Fig. 1(d) has been suggested for these systems^{15,16,17,18}. Within this picture, each dimer unit cell acts as a single site in an *effective* spin 1/2 rectangular ladder with significant spin gap (see below). The mapping from the dimerized 1/4-filled band electron model to the spin model, or the occurrence of spin gap in the original 1/4-filled band model have, however, not been demonstrated.

Yet another 1/4-filled band ladder system in which relatively large spin gap (34 K) has been observed is $\alpha'\text{-NaV}_2\text{O}_5$, which consists of V-O ladders coupled through weak V-V bonds, with the V-O layers separated by layers of Na^+ ions²¹. Charge order involving the V

sites and spin gap occur at the same temperature in this system.²¹ Theoretical description based on the V-only 1/4-filled d-band extended Hubbard model predict the checkerboard charge-order pattern of Fig. 1(c). for the V-ladders.^{22,23} The calculated spin gap within the checkerboard charge-order phase for hopping parameter $t_{\perp} > t$, as is appropriate^{22,23} for $\alpha\text{-NaV}_2\text{O}_5$, is however zero¹¹. The spin gap here most likely originates from the coupling between the 1/4-filled ladders^{23,24,25,26}, which can lead to effective dimerization along the legs of the individual ladders with the checkerboard charge order (see below).

In view of the interest in theoretical models for coupled 1/4-filled band two-chain systems that give large spin gaps, we have performed DMRG calculations for the 1/4-filled band rectangular ladder with leg-bond dimerization within the extended Hubbard model. The purpose of our work is not necessarily to explain the observed experimental behavior of the organic charge-transfer solids or $\alpha'\text{-NaV}_2\text{O}_5$, but to determine the plausibility of the application of the models to these systems. The minimum requirement of the applicability of the model is that significant spin gap occurs within it for realistic rung hopping parameter t_{\perp} . We have considered two distinct parameter regimes, (i) $V < V_C(U)$, corresponding to homogenous charge distribution on the sites, and (ii) $V > V_c(U)$, which gives the checkerboard charge order in the infinite ladder.¹¹ In (i), we have considered mostly hopping parameter $t_{\perp} \leq t$, as the results for larger t_{\perp} are easily anticipated from these calculations. In (ii) we have considered hopping parameter $t_{\perp} \geq t$ because of the possible applicability of to $\alpha'\text{-NaV}_2\text{O}_5$, in which the rung hopping is larger than the hopping along the leg bonds. In both cases we find spin gaps that are nearly an order of magnitude larger than those in the undimerized ladders.

The paper is organized as follows. In section II we present the theoretical model and methodology. In section III we show the numerical results for the two cases, nearest neighbor electron-electron interaction $V < V_C(U)$ and $V > V_c(U)$. Finally, in section IV we present our conclusions and discuss possible applications of the present work to the 1/4-filled band paired-stack charge-transfer solids and $\alpha'\text{-NaV}_2\text{O}_5$.

II. THEORETICAL MODEL AND METHODOLOGY

We have performed DMRG calculations for the dimerized rectangular ladder of Fig. 1(d), within the Hamiltonian,

$$\begin{aligned}
H = & U \sum_i n_{i,\lambda,\uparrow} n_{i,\lambda,\downarrow} + V \sum_{i,\lambda=-1,+1} n_{i,\lambda} n_{i+1,\lambda} \\
& + V_{\perp} \sum_i n_{i,1} n_{i,-1} \\
& + t \sum_{i,\sigma,\lambda=-1,+1} (1 \pm \delta) (c_{i,\lambda,\sigma}^{\dagger} c_{i+1,\lambda,\sigma} + h.c.) \\
& + t_{\perp} \sum_{i,\sigma} (c_{i,1,\sigma}^{\dagger} c_{i,-1,\sigma} + h.c.)
\end{aligned} \tag{1}$$

Here $c_{i,\lambda,\sigma}^{\dagger}$ creates an electron with spin $\sigma = \uparrow, \downarrow$ on site i in ladder leg $\lambda = \pm 1$, $n_{i,\lambda,\sigma} = c_{i,\lambda,\sigma}^{\dagger} c_{i,\lambda,\sigma}$, and δ is the bond-alternation parameter along the legs. The parameters $U, V, V_{\perp}, t, t_{\perp}$ have their usual meanings. In the following we present all quantities with dimensions of energy in units of hopping parameter t . We are interested in the parameter space $U > V, V_{\perp} \geq 0$, and only in possible spin gap, as the conditions for charge gap and charge order have been discussed extensively in previous work^{9,11}. For simplicity, we present results for $V = V_{\perp}$ and refer to both interactions as V . The spin gap Δ_S is defined as usual as $E(1) - E(0)$, where $E(S)$ is the lowest energy in the state with total spin S . Note that for the 1/4-filled band spin gap $\Delta_S = 0$ for hopping parameter $t_{\perp} = 0$ even with bond-alternation parameter $\delta \neq 0$. Although we are mostly interested in determining whether the spin gap is nonzero for arbitrarily small hopping parameter t_{\perp} and bond-alternation parameter δ , our calculations span both $t_{\perp} < 1$ and $t_{\perp} > 1$.

Before discussing our numerical results we present here brief discussions of the the physical mechanism behind the opening up of the spin gap in the dimerized ladder. Consider first the $U, V, V_{\perp} = 0$ band limit of Eq. 1. The electronic structure in this limit and for bond-alternation parameter $\delta = 0$ is given by noninteracting bonding and antibonding bands split by $2t_{\perp}$. For $t_{\perp} < 1$ and bandfilling of 1/4, electrons occupy both bands and there are four Fermi points. For $t_{\perp} > 1$, the lower band is 1/2-filled and the upper band empty. $U > 0$ introduces a charge gap now, but the spin gap continues to be zero. Nonzero leg bond dimerization $\delta \neq 0$ in the limit $U, V, V_{\perp} = 0$ opens a gap at the wavevector $k = \pi/2a$ (where a = lattice spacing in the ladder leg direction). For small t_{\perp} and bond-alternation parameter δ , both bands are again occupied. For $t_{\perp} \sim 1$ now there appears a charge and spin gap $2(t_{\perp} - 1 + \delta)$ in the spectrum. For $t_{\perp} \gg 1$, the energy gap at the Fermi surface in the bonding band is 4δ . These known results suggest that there exists a range of t_{\perp} and

δ where the spin gap can conceivably be significant for nonzero U, V, V_{\perp} .

The above physical picture does not explain the logic behind the proposed relationship between the dimerized 1/4-filled band model of Eq. (1) and the spin or 1/2-filled band ladders.^{15,16,17,18} This can be understood starting from a different limit, large bond-alternation parameter $\delta \sim 1$. In this limit each dimer unit forms a molecule with bonding and antibonding molecular orbitals (MOs) at energy $\pm 2t$. The single electron within each dimer molecule occupies the bonding MO, which forms an effective single site, as the unoccupied antibonding MO is too high in energy and does not play significant role in the low energy behavior of the system. The singly occupied bonding MOs, coupled through the weak intersite leg bonds and the rung bonds then constitute the effective sites of a 1/2-filled band ladder, for which we expect nonzero spin gap for arbitrarily small hopping parameter t_{\perp} . Whether or not the spin gap is nonvanishing also for small δ can be found only numerically. We will show that the spin gaps that we obtain numerically are considerably more enhanced compared to those obtained in the $U = V = 0$ limit, viz., $2(t_{\perp} - 1 + \delta)$ for $t_{\perp} \sim 1$ and 4δ for $t_{\perp} \gg 1$. We will also show that the U-dependence of the spin gaps for the dimerized 1/4-filled band ladder are very similar to those of the 1/2-filled band ladder.

We calculated the spin gap for rectangular ladders up to 2×64 sites using the infinite-system DMRG algorithm with open boundary condition. Instead of a single site, a single rung is added to the building block each time. The number of states we keep is $m = 300$ for the $S=0$ state and 600 for the $S=1$ state. We have confirmed that the accuracy of the singlet state is comparable to that of the triplet with these m . We checked some of our results against published results,⁹ and found that the errors in our calculations are comparable, estimated to be less than a few percent.

In principle, our calculations should be done with the finite-system DMRG algorithm, which is known to be more accurate than the infinite-system DMRG algorithm. The former procedure, however, requires considerably larger amount of time for each different ladder size and parameter set. The particular problem we consider requires that calculations are done with many different U, V, t_{\perp} and bond-alternation parameter δ (see below), with multiple system sizes L for effective $L \rightarrow \infty$ extrapolations. The enormous amount of computational time that would be necessary for performing all the calculations that are reported below makes the finite-system DMRG algorithm impractical in the present case. We note, however, that in nearly all the cases we discuss below the calculated spin gaps are large and easy to

detect. We also note that the primary purpose of our work is to determine whether or not significant spin gaps are obtained within the dimerized ladder, and the precision required is not the same as within models where the gaps are tiny.¹¹ We have calculated a few of the spin gaps for several different system sizes, for representative parameters that cover both $V < V_c(U)$ and $V > V_c(U)$ within the finite-system DMRG algorithm using the same number of states as the infinite-system algorithm, and we compare these values with those obtained with the infinite-system algorithm in Table 1. As seen from the Table, the accuracies of the infinite-system algorithm are acceptable for our purpose, in both parameter regimes.

III. NUMERICAL RESULTS

A. Case 1. $V < V_c(U)$

In Fig. 2(a) we show our calculated spin gap Δ_S for 1/4-filled $2 \times L$ ladders, for the representative case of $U = 8$, $V = 0$, $t_\perp = 1$ and $0 \leq \delta \leq 0.05$. For this moderately large t_\perp , the accuracy of the numerical results is very high and reliable results are obtained for the smallest bond-alternation parameter δ . The kink in the spin gap Δ_S plot for bond-alternation parameter $\delta = 0.05$ is real, - similar behavior has been seen previously for the undimerized 1/4-filled band ladder (see Fig. 3 in reference 11). The dashed lines indicate the $L \rightarrow \infty$ extrapolations of the spin gaps, obtained by fitting the calculated spin gap Δ_S against a polynomial in $1/L$ up to $1/L^2$. For bond-alternation parameter $\delta = 0.02$ and 0.05 , we have also performed the extrapolations by retaining terms up to $1/L^3$. The two different extrapolations in each of these cases give the uncertainties in the spin gaps, which are 0.121 ± 0.008 and 0.244 ± 0.015 respectively. For all other cases fittings with $1/L$ alone gave extrapolations that are indistinguishable from the plots shown on the scale of the figure. The $L \rightarrow \infty$ extrapolated spin gap for bond-alternation parameter $\delta = 0$ is zero in Fig. 2(a), in agreement with previous work.¹¹ For bond-alternation parameter δ as small as 0.01 , the extrapolated spin gap Δ_S is nonzero for $t_\perp = 1$. Furthermore, for this t_\perp the spin gap at $U = 0$ is 2δ . As seen in the Fig., for all bond-alternation parameter δ , the extrapolated spin gap Δ_S for $U = 8$ is larger. We therefore conclude that the spin gap is enhanced by the on-site e-e interaction, and is hence nonzero for the smallest bond-alternation parameter δ at $t_\perp = 1$. The inset in Fig. 2(a) shows the weakly sublinear behavior of spin gap Δ_S against

bond-alternation parameter δ .

Unfortunately, as the system size approaches the thermodynamic limit, the spin gap Δ_S decreases at smaller t_\perp and the numerical accuracy of the DMRG results at large L are reduced. This has also been seen in previous calculations.^{9,11} Even for the relatively simpler case of the 1/2-filled Hubbard ladder precise calculations of the spin gap are difficult for $t_\perp < 1$.⁹ Our calculations of the spin gap for the smaller $t_\perp = 0.8$ in Fig. 2(b) are therefore for moderate bond-alternation parameter $\delta \geq 0.05$. Considering that at $U = 0$ the spin gap $\Delta_S = 2(t_\perp - 1 + \delta)$ are zero for bond-alternation parameter $\delta \leq 0.2$, we see that the extrapolated spin gaps are once again strongly enhanced by U . Taken together with the weak-coupling result that the spin gap is nonzero (albeit small) for all $t_\perp < 1$ at $\delta = 0$,¹³ the results of Fig. 2(a) and (b) suggest that for nonzero δ and U the spin gap is nonzero for all t_\perp . The main difference between $\delta = 0$ and $\delta \neq 0$ is that the spin gap in the latter case is largest for $t_\perp \geq 1$, exactly the region where the spin gap is zero for $\delta = 0$. The appearance of nonzero spin gap for the smallest bond-alternation parameter δ indicates that there is indeed a qualitative similarity between the the 1/4-filled band dimerized rectangular ladder and an effective spin ladder.

In Fig. 2(c) we have shown the effect of nonzero V on the spin gap for $U = 8$ and $t_\perp = 0.8$ and bond-alternation $\delta = 0.05$. V enhances the spin gap very strongly, such that even for $t_\perp = 0.8$ the spin gap is now quite large. The enhancement of the spin gap due to V can be understood physically, given the δ -dependence of spin gap Δ_S . Defining the bond-orders along the ladder legs in the usual manner, $B_{i,\lambda} = \langle c_{i,\lambda,\sigma}^\dagger c_{i+1,\lambda,\sigma} + h.c. \rangle$, we note that for nonzero bond-alternation δ the absolute value of the difference between consecutive bond orders, $\Delta B = |B_{i,\lambda} - B_{i+1,\lambda}| > 0$. ΔB is then a *wavefunction measure of leg bond-dimerization*,¹⁴ and for fixed bond-alternation δ we expect the spin gap to increase with ΔB . We have calculated the exact $\Delta B(V)$ at fixed $U = 8$ for finite 1/4-filled periodic 1D rings and ladders with $t_\perp = 0.0$ and 0.8 with 12 and 16 sites. In Fig. 2(d) we have plotted $\Delta B(V)/\Delta B(0)$ for $U = 8$ against V . As a consequence of the well known 4n vs. 4n+2-electron effect, we expect the curves for the infinite system to be bounded by the curves for the 12- and 16-site periodic systems for both t_\perp . The enhancement of $\Delta B(V)$ with V indicates enhanced effective leg bond-dimerization with V . Thus V increases the spin gap because it increases the dimerized nature of the ground state wavefunction. For $U = 8$, the checkerboard charge order of Fig. 1(c) is obtained¹¹ for $V > V_c(U) \simeq 2.6$ at bond-alternation

parameter $\delta = 0$.¹¹ Our calculations in Fig. 2(c) and (d) are for $V < V_c(U)$. We discuss $V > V_c(U)$ separately.

In order to get more complete understanding of the behavior of the spin gap within Eq. 1 we have calculated the $L \rightarrow \infty$ extrapolated spin gaps for several sets of U , V , t_\perp and δ . The parameter region of large $t_\perp > 1$ and large $\delta > 0.2$ will clearly yield large spin gaps and is hence uninteresting. We are interested primarily in the $t_\perp < 1$ region, thought to be applicable to the organic charge-transfer solids.^{15,16,17,18} Also in the context of the charge-transfer solids, $\delta \leq 0.1$.²⁸ In Fig. 3(a) we have plotted the extrapolated spin gaps Δ_S versus t_\perp for several different U , but $V = 0$, for bond-alternation parameter $\delta = 0.05$. Because of the large uncertainties in the calculated Δ_S for small t_\perp our results in Fig. 3(a) are limited to $t_\perp \geq 0.6$. The results for the same U but larger bond-alternation $\delta = 0.1$ are shown in Fig. 3(b). Fig. 3(c) shows the spin gap behavior for fixed $U = 8$, with three different $V < V_c(U)$. In all cases, and for all t_\perp we find considerable enhancement of the spin gap by e-e interactions, as is summarized in Fig. 3(d). The behavior of the spin gap as a function of U in Fig. 3(d) is qualitatively similar to that of the uniform 1/2-filled band rectangular Hubbard ladder (see Fig. 4 in reference 9), suggesting again that the spin excitations of the dimerized 1/4-filled rectangular ladder can be obtained from those of the rectangular spin-ladder (note that increasing atomic U also increases the Coulomb repulsion between two electrons occupying the same bonding MO of the dimer unit²⁷. It has been claimed that such mapping can give rung spin exchange in the effective spin ladder larger than the nearest neighbor spin exchange along the legs, even for smaller hoppings along the rungs within the quarter-filled band electron ladder.^{15,16,17} For the dimerized linear chain the transformation from the atomic basis to the dimer MO basis²⁷ gives $t/2$ as the effective hopping between dimer MOs along the chain. This remains true here for the leg bonds. On the other hand, within the atomic basis of Eq. (1), there are two rung hoppings between the dimer units. The overall rung hopping between the dimer bonding MOs then continues to be t_\perp after transformation to the dimer MO basis. Hence for all rung hopping $t_\perp \geq 0.5$ in the 1/4-filled ladder the rung spin exchange in the effective spin ladder is larger than the leg spin exchange. We have confirmed this numerically: the $L \rightarrow \infty$ spin gap of the 1/4-filled band ladder at a fixed U with any specific t_\perp/t is reproduced in the 1/2-filled band ladder with same U for much larger t_\perp/t .

B. Case 2. $V > V_c(U)$

The calculations reported in the above are for $V < V_c(U)$ and $t_\perp \leq 1$. For $V > V_c(U)$ and $U, V \gg 1$, the checkerboard charge order of Fig. 1(c) is obtained in the infinite ladder, while in finite systems there occur charge-charge correlations corresponding to this charge order.¹¹ The “occupied” sites in Fig. 1(c) behave as charge e particles with spin 1/2. At $\delta = 0$, nonzero spin gap can occur only for small t_\perp , where a spontaneous Majumdar-Ghosh dimerization spin gap^{5,6,7,8} opens up.¹¹ There can, however, be no spin gap in this case for $t_\perp \geq 1$. The situation is different for nonzero δ , as indicated in our numerical results for large $t_\perp = 1$ in Fig. 4 (a). $V_c(U)$ here for $\delta = 0$ is 2.6¹¹, and nonzero δ is expected to slightly enhance $V_c(U)$. For $t_\perp = 1$, we find then coexistence of the checkerboard charge order and spin gap in the region $3 \leq V \leq 4$. With even larger $t_\perp = 2$ the spin gap varies only weakly with V . The energy gap between the bonding and antibonding dimer MOs are now very large, and the system behaves here as a simple 1D dimerized Heisenberg chain.

The width of the region over which there occurs coexistence of charge order and spin gap clearly depends on the bond-alternation. Indeed, had we performed our calculations self-consistently with e-p couplings that modulated the hopping integrals along the leg bonds, as opposed to with rigid bond-alternation δ , the amplitude of the bond-dimerization would have decreased with V in the $V > V_c(U)$ region and the coexistence region would have been narrower. This is known from calculations within the 1D 1/4-filled band e-p coupled extended Hubbard model where the bond dimerization decreases with V in the region $V > V_c(U)$ ²⁸. The same physics can also be captured from calculations of the bond orders $B(V)$. In Fig. 4(b) we show plots of $\Delta B(V)/\Delta B(0)$ for the parameters of Fig. 4(a), obtained from exact diagonalizations of 12 and 16-site periodic ladders with 6 and 8 electrons, respectively. As in Fig. 2(d), the plots for the infinite system are expected to lie in between the curves for the 12 and 16-site ladders for each t_\perp . Thus for the infinite ladder, the bond order difference is expected to first increase with V at $t_\perp = 1$ up to $V \sim 2$, following which it is expected to decrease in the $2 < V < 4$ region. Similarly, for $t_\perp = 2$ the bond order difference is expected to be nearly flat in this region of V , with the decrease occurring at even larger V . In both cases, the qualitative behavior of the bond order differences and the spin gaps are the same, emphasizing the strong role of the leg bond dimerization. Similar relationship between the dimerization and the spin gap has also been observed in a recent calculation

on coupled ladders, where the effective dimerization is a consequence of the charge order on neighboring ladders.²⁶

IV. DISCUSSIONS AND CONCLUSIONS

In summary, the spin gap within the 1/4-filled band rectangular correlated-electron ladder is nonzero for the smallest bond-alternation, and increases monotonically with rung hopping t_{\perp} in the region $0 < t_{\perp} < 1$. The qualitative similarity between the dimerized 1/4-field band ladder and the spin ladder is easily understood in the large bond-alternation region, and persists at smaller bond-alternation, as is seen from the enhancement of the spin gap by dimerization, and the enhancement of the spin gap by both U and V for $V < V_c(U)$ at fixed dimerization. For $V > V_c(U)$, there can be coexistence of charge order and spin gap, especially for large $t_{\perp} > 1$.

In the context of the charge-transfer solids, the electronic parameters appropriate for quasi-1D cationic systems are known to be²⁸ $t \sim 0.1$ eV, $U/t \sim 6 - 8$ and $V \sim 2t < V_c(U)$. Assuming similar intrastack parameters for the paired-stack charge-transfer solids, the very large T_{SG} in these indicate spin gap $\Delta_S \geq 0.2$. Assuming that the bond-dimerization $\delta \sim 0.1$, as is true in most quasi-1D charge-transfer solids²⁸, we see from Fig. 3 that such large spin gaps are obtained only for $t_{\perp} \geq 0.8$, and certainly $t_{\perp} < 0.7$ is impossible. Somewhat larger spin gap is obtained within the 1/4-filled band zigzag ladder for realistic e-e and e-p interaction parameters¹⁴, but the BCDW here appears only for $t_d \geq 0.6$. Thus both the electron ladder models would require substantial interchain hopping to give the observed large spin gaps. The difference between the two models is that while no charge order is expected within the rectangular ladder model for the charge-transfer solids, spin gap in the zigzag ladder is accompanied by strong charge order. Experiments that probe charge disproportionation are required to determine which of the two models apply to the real materials.

As regards α' -NaV₂O₅, our numerical results of Fig. 4(a) are in agreement to the conclusions of references 25 and 26. As shown in these papers, because of the coupling between the ladders in α' -NaV₂O₅, the charge order can drive effective bond dimerization along the ladder legs that is manifested in the alternation of intraladder coupling parameters (there is a subtle difference between reference 25, which models α' -NaV₂O₅ as a system with charge

order on only alternate ladders and reference 26 which assumes charge order in every ladder; this difference is not important in the present context.) The spin gaps in these references are explained within coupled dimerized spin chain models. DMRG calculations within the extended Hubbard model for two coupled ladders with charge order also find spin gap up on extrapolation²⁶, but by necessity the maximum ladder length (20 rungs) is small here. Our calculations are thus complementary to previous work, showing that once it is assumed that interladder coupling gives rise to effective bond dimerization the essential physics is captured within the electronic Hamiltonian for the single ladder.

V. ACKNOWLEDGMENTS

S.M. acknowledges useful discussions with R. Torsten Clay and J. Musfeldt. This work was supported by the NSF-DMR-0406604, NSF-INT-0138051 and DST, India through /INT/US(NSF-RP078)/2001.

-
- ¹ E. Dagotto and T.M. Rice, *Science* **271** , 618 (1996).
- ² T. Barnes, E. Dagotto, J. Riera and E. S. Swanson, *Phys. Rev. B* **47**, 3196 (1993).
- ³ S.R. White, R.M. Noack and D.J. Scalapino, *Phys. Rev. Lett.* **73**, 886 (1994).
- ⁴ S. Gopalan, T.M. Rice and M. Sigrist, *Phys. Rev. B* **49**, 8901 (1994).
- ⁵ T. Tonegawa and I. Harada, *J. Phys. Soc. Jpn.* **56**, 2152 (1987).
- ⁶ R.J. Bursill, G. A. Gehring, D. J. J. Farnell, J. B. Parkinson, T. Xiang and C. Zeng, *J. Phys. Condens. Matter* **7**, 8605 (1995).
- ⁷ R. Chitra, Swapan Pati, H. R. Krishnamurthy, Diptiman Sen and S. Ramasesha, *Phys. Rev. B* **52**, 6581 (1995).
- ⁸ S.R. White and I. Affleck, *Phys. Rev. B* **54**, 9862 (1996).
- ⁹ R.M. Noack, S.R. White and D.J. Scalapino, *Physica C* **270**, 281 (1996).
- ¹⁰ E. Dagotto, *Reports on Progress in Physics* **62**, 1525 (1999). The observed superconductivity in the cuprate ladder materials $(\text{La},\text{Y},\text{Sr},\text{Ca})_{14}\text{Cu}_{24}\text{O}_{41}$ is, however, probably unrelated to the theoretical models of superconductivity in doped spin ladders. See, T. Vuletic, B. Korin-Hamzic, T. Ivetk, S. Tomic, B. Gorshunov, M. Dressel and J. Akimitsu, *Phys. Rep.*, to be published.

- ¹¹ M. Vojta, A. Hübsch and R.M. Noack, Phys. Rev. B **63**, 045105 (2001).
- ¹² J. Riera and D. Poilblanc, Phys. Rev. B **59**, 2667 (1999).
- ¹³ L. Balents and M..A. Fisher, Phys. Rev. B **53**, 12133 (1996).
- ¹⁴ R.T. Clay and S. Mazumdar, Phys. Rev. Lett. **94**, 207206 (2005).
- ¹⁵ X. Ribas, M. Mas-Torrent, A. Perez-Benitez, J. C. Dias, H. Alves, E. B. Lopes, R. T. Henriques, E. Molins, I. C. Santos, K. Wurst, P. FouryLeylekian, M. Almeida, J. Veciana and C. Rovira, Adv. Funct. Mater. **15**, 1023 (2005).
- ¹⁶ E. Ribera, C. Rovira, J. Veciana, J. Tarres, E. Canadell, R. Rousseau, E. Molins, M. Mas, J. Schoeffel, J. Pouget, J. Morgado, R. T. Henriques, M. Almeida and E. Ribera, Chem. Eur. J. **5**, 2025 (1999).
- ¹⁷ R. Wesolowski, J. T. Haraldsen, J. L. Musfeldt, T. Barnes, M. Mas-Torrent, C. Rovira, R. T. Henriques and M. Almeida, Phys. Rev. B **68**, 134405 (2003).
- ¹⁸ T. Nakamura, K. Takahashi1, T. Shirahata2, M. Uruichi, K. Yakushi and T. Mori, J. Phys. Soc. Jpn. **71**, 2022 (2002).
- ¹⁹ J.P. Pouget and S. Ravy, Synth. Metals **85**, 1523 (1997).
- ²⁰ R. J. J. Visser, S. Oostra, C. Vettier and J. Voiron., Phys. Rev. B **28**, 2074 (1983).
- ²¹ M. Isobe and Y. Ueda, J. Phys. Soc. Jpn. **65**, 1178 (1996).
- ²² H. Seo and H. Fukuyama, J. Phys. Soc. Jpn. **67**, 2602 (1998).
- ²³ M.V. Mostovoy and D.I. Khomskii, Solid St. Commun. **113**, 159 (2000).
- ²⁴ H. Smolinski, C. Gros, W. Weber, U. Peuchert, G. Roth, M. Weiden and C. Geibel, Phys. Rev. Lett. **80**, 5164 (1998) and references therein.
- ²⁵ A. Bernert, P. Thalmeier and P. Fulde, Phys. Rev. B **66**, 165108 (2002) and references therein.
- ²⁶ B. Edegger, H.G. Evertz and R.M. Noack, cond-mat/0510325 and references therein.
- ²⁷ M. Chandross, Y. Shimo and S. Mazumdar, Phys. Rev. B **59**, 4822 (1999).
- ²⁸ R.T. Clay, S. Mazumdar and D.K. Campbell, Phys. Rev. B **67**, 115121 (2003).

TABLE I: Spin gaps obtained by using the infinite-system and finite-system DMRG algorithms.

 In all cases $U=8$.

Parameters	L	spin gap Δ_s	
		infinite	finite
$V=0$	40	0.178337	0.177095
	48	0.165737	0.164359
	56	0.157386	0.155845
	64	0.151652	0.149933
	∞	0.121 ± 0.008	0.111 ± 0.006
$V=2$	40	0.235359	0.234463
	48	0.234640	0.233727
	56	0.234241	0.233316
	64	0.234000	0.233068
	∞	0.233 ± 0.001	0.232 ± 0.001
$V=3$	40	0.166847	0.166470
	48	0.162380	0.161969
	56	0.159576	0.159126
	64	0.157700	0.157209
	∞	0.146 ± 0.003	0.145 ± 0.003

Figure Captions

Figure 1. Quarter-filled band two-leg electron ladders. Grey, black and white circles represent mean electron occupations 0.5, > 0.5 and < 0.5 , respectively. (a) Rectangular ladder with hopping integrals t and t_{\perp} along the leg and the rung, respectively. (b) The BCDW broken symmetry in the 1/4-filled zigzag ladder, with average intrastack and interstack hopping integrals t_s and t_d , respectively. (c) The checkerboard charge order in the 1/4-filled band rectangular ladder. (d) The bond-dimerized 1/4-filled band rectangular ladder.

Figure 2 (a) and (b) Convergence behavior of spin gaps for the 1/4-filled band dimerized rectangular ladder for $U=8$ and $V=0$. In (a) the rung hopping parameter $t_{\perp}=1$, the maximum number of rungs $L_{max}=80$; \circ , \triangle , \square and \diamond correspond to bond-alternation parameter $\delta=0, 0.01, 0.02$ and 0.05 , respectively. In the curves corresponding to $\delta=0.02$ and 0.05 , the upper $L \rightarrow \infty$ extrapolation is using polynomial in $\frac{1}{L}$ up to $\frac{1}{L^3}$ and the lower one up to $\frac{1}{L^2}$.

In (b), $t_{\perp}=0.8$; \diamond , $+$ and \times correspond to $\delta=0.05, 0.1$ and 0.2 , respectively. (c) Spin gaps for $U=8, t_{\perp}=0.8, \delta=0.05$, with different V . \diamond , \blacktriangle and \blacksquare correspond to $V=0, 1$ and 2 , respectively. (d) The normalized absolute difference in consecutive bond orders, $\Delta B(V)/\Delta B(0)$, as a function of V for $U = 8$. Here \circ and \square correspond to periodic rings with 12 and 16 sites (i.e., $t_{\perp}=0$ in Eq. 1 and $\delta=0.05$), respectively; the \bullet and \blacksquare to ladders with 12 and 16 sites ($t_{\perp}=0.8, \delta=0.1$) respectively. In all cases the number of electrons is half the number of sites.

Figure 3 (a) DMRG $L \rightarrow \infty$ spin gaps versus rung hopping t_{\perp} for different U , for bond-alternation $\delta=0.05$. (b) Same for $\delta=0.1$. (c) Same for fixed $U=8$ with different V . (d) Extrapolated spin gaps at $\delta=0.05$ versus U , for three different t_{\perp} . \bullet and \blacksquare correspond to $V=1$ for rung hoppings $t_{\perp}=0.8$ and $t_{\perp}=1$.

Figure 4. (a) $L \rightarrow \infty$ spin gaps versus V for $U=8, \delta=0.05$ and two values of t_{\perp} . For $V \geq 3$ the spin gap coexists with the checkerboard charge order. (b) The normalized absolute difference in consecutive bond orders; The \circ and \square correspond to 12 and 16-site ladders, respectively, at $t_{\perp}=1$. The \bullet and \blacksquare correspond to 12 and 16-site ladders, respectively, at $t_{\perp}=2$.

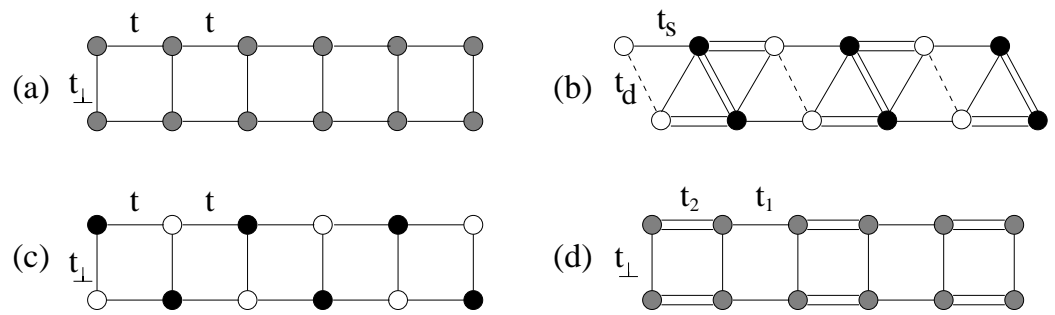


FIG. 1:

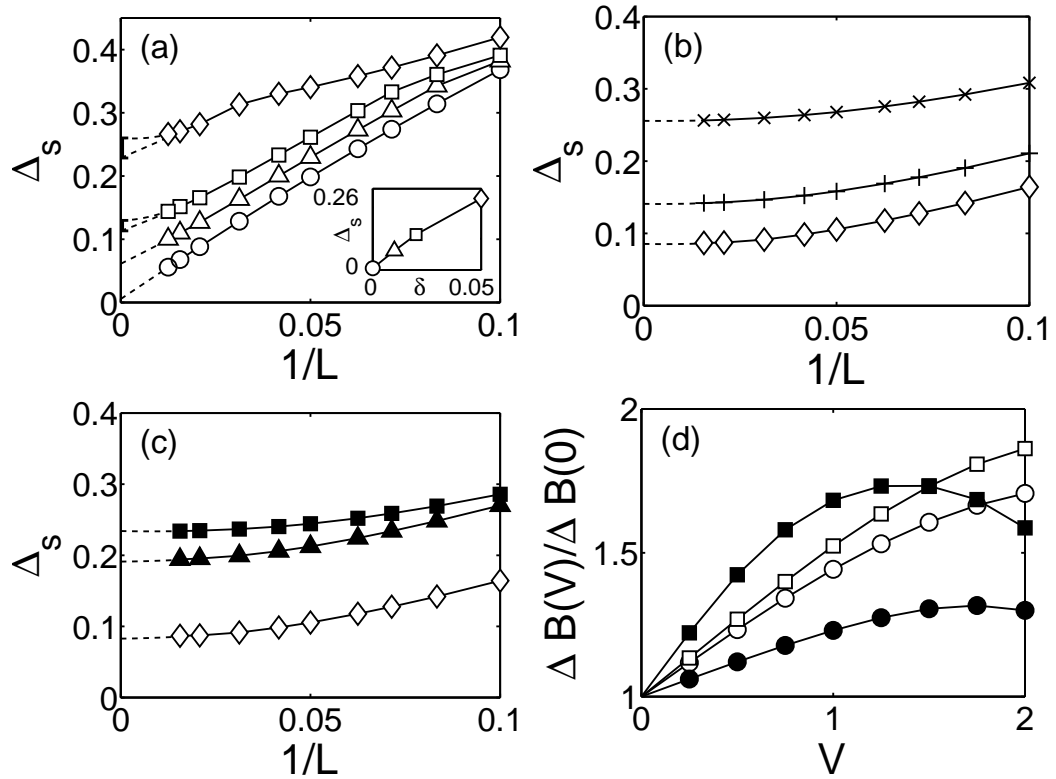


FIG. 2:

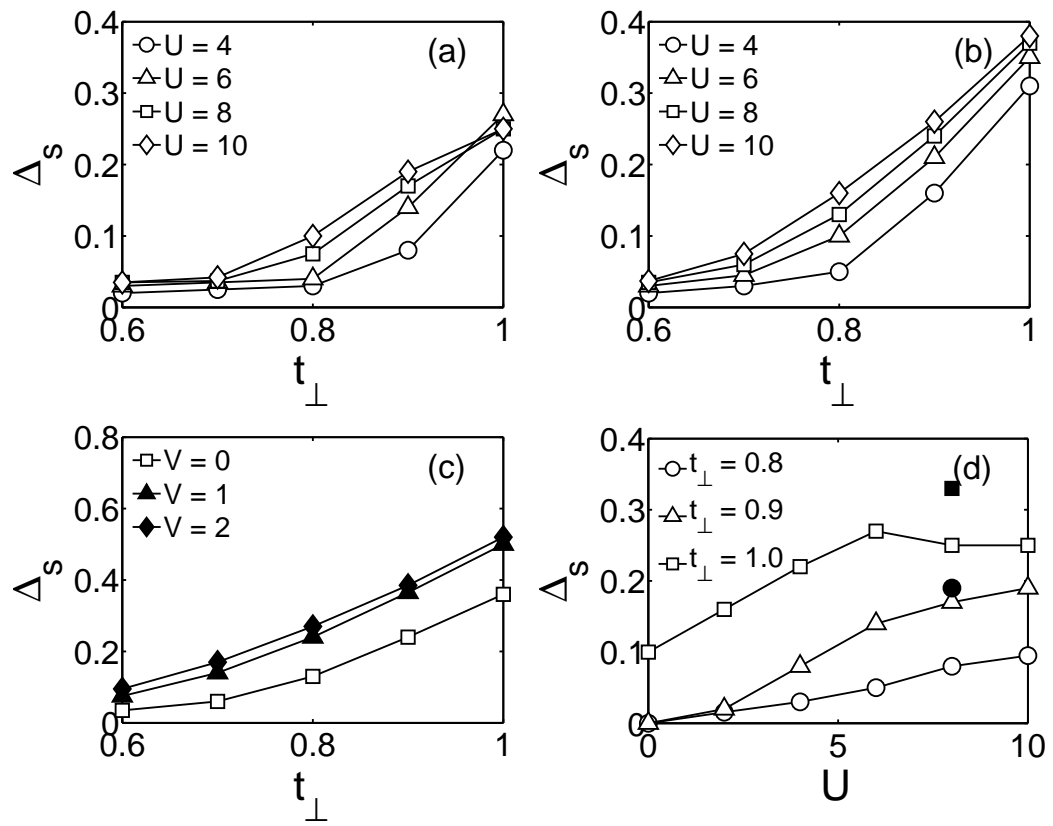


FIG. 3:

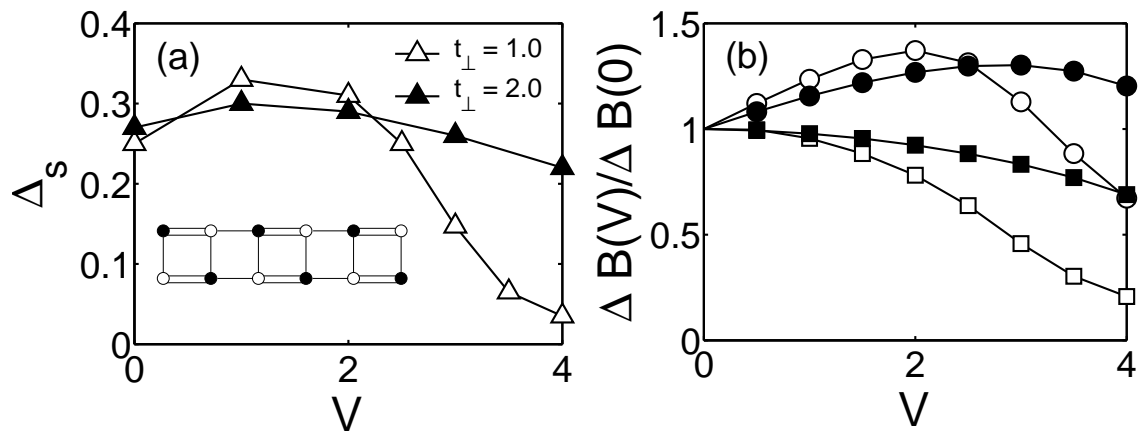


FIG. 4: